Letter

Multipoint fishnet Feynman diagrams: Sequential splitting

Francesco Aprile[1] and Enrico Olivucci[2]

[1]*Departamento de Física Teórica and IPARCOS, Facultad de Ciencias Físicas, Universidad Complutense de Madrid, 28040 Madrid, Spain*

[2]*Perimeter Institute for Theoretical Physics, Waterloo, Ontario N2L 2Y5, Canada*

(Received 20 September 2023; accepted 27 November 2023; published 21 December 2023)

We study fishnet Feynman diagrams defined by a certain triangulation of a planar n-gon, with massless scalars propagating along and across the cuts. Our solution theory uses the technique of separation of variables, in combination with the theory of symmetric polynomials and Mellin space. The n-point split-ladders are solved by a recursion where all building blocks are made fully explicit. In particular, we find an elegant formula for the coefficient functions of the light-cone leading logs. When the diagram grows into a fishnet, we obtain new results exploiting a Cauchy identity decomposition of the measure over separated variables. This leads to an elementary proof of the Basso-Dixon formula at 4-points, while at n-points it provides a natural operator product expansion-like stratification of the diagram. Finally, we propose an independent approach based on "stampede" combinatorics to study the light-cone behavior of the diagrams as the partition function of a certain vertex model.

DOI: 10.1103/PhysRevD.108.L121902

Introduction. Feynman diagrams [1] are central for our understanding of Nature at the quantum level. The case of collider physics is a perfect example of this paradigm. However, diagrams are often hard to compute and alternative routes are needed in the study of a relativistic quantum process. In this paper we embrace this point of view and use an integrability-based technique, known as separation of variables (SoV), to study a class of *multipoint* Feynman diagrams in $4d$, whose complexity depends on a *fishnet* of massless scalar propagators. Our diagrams lie on a *planar* triangulation of an n-gon, and their SoV representation can be obtained by gluing together objects assigned to triangles. The general pattern is presented in [2]. Here we will focus on splitting a 4pt triangulation sequentially, so to generate a particular class of Feynman diagrams. See Figs. 1–3.

While the SoV representation is not new [3–6], some practical challenges with it remained unexplored until now, especially for $n \geq 5$. First, each triangle carries an R-matrix tensor structure contribution from the underlying spin-chain formalism. Second, for higher-pts there are many possible configurations of propagators. Third, there is a variety of kinematical limits $x_{ij}^2 \to 0$ that one might want to consider. In this situation, what we expect from SoV is the ability to make manifest new structures, otherwise hidden in the Feynman representation, and the ability to provide data in a simple way, e.g. by expansions around light-cone limits. At 4pt all of this is well established. Indeed, the SoV representation allowed [4] to prove the conjecture of [7] about rectangular fishnets being equal to determinants of ladder integrals.

In this paper we set the stage for investigating emergent structures in multi-point fishnet diagrams that lie on the plane. First, we shall understand the simplest diagrams, i.e., split-ladders. Second, we will massage the SoV representation so to make it as explicit as possible. For the first task, we will show that the integration of n-pt split ladders reduces to a recursion, and that the relevant R-matrix construction admits a simple closed-form expression. Remarkably, the coefficient functions of the light-cone leading logs is expressed as a rational factor times a combination of multiple polylogarithms (MPLs) taking the elegant form

$$\frac{\texttt{MPLs}}{(W_{n-3}-\bar{W}_{n-3})}=\sum_{\substack{a_2\in\mathbb{N}\\ \cdots\\ a_{n-3}\in\mathbb{N}}}\prod_{i\geq 2}\frac{\mathcal{D}_{i,i-1}^{(a_i)}}{a_i^{L_i}}\left[\frac{\mathrm{Li}_{L_1}(W_1)-\mathrm{Li}_{L_1}(\bar{W}_1)}{W_1-\bar{W}_1}\right] \tag{1}$$

where

$$\mathcal{D}_{i,i-1}^{(a_i)}=\frac{(-\bar{W}_i\partial_{\bar{W}_{i-1}}-W_i\partial_{W_{i-1}})^{a_i-1}}{(a_i-1)!}. \tag{2}$$

and the index $i=2,\ldots,n-3$. The variables W_i will parametrize spacetime cross-ratio, as we explain later, and the function $\mathrm{Li}_k(x)$ is the classical polylogarithm function.

For the second task, we will present a Cauchy identity decomposition of the SoV measure that makes transparent the derivation of the 4pt determinant of [7,8], and paves the way to the understanding of the n-pt split-fishnet diagrams. Finally, we make an intriguing observation inspired by stampede methods [9] that relates the coefficient functions of the light-cone leading logs with the partition function of some vertex model.

SoV diagrammatic rules. Draw an n-gon *on the plane* and a triangulation of it into $n-2$ triangles. Edges between non-adjacent external points cut the diagram, and are $n-3$. To each cut assign an integer L_j, that counts propagators along the cut, and another integer M_j, that counts propagators across the cut. For illustration see Fig. 1.

The SoV representation of such diagrams is a certain integral that can be read from the following set of rules. The j-th cut carries rapidities $\mathbf{u}_j = (u_{j_1}, \ldots, u_{j_{M_j}})$ and quantum numbers $\mathbf{a}_j = (a_{j_1}, \ldots, a_{j_{M_j}})$. Here $u \in \mathbb{R}$, while $a \in \mathbb{N}$ labels an $su(2)$ rep V_a of spin $\frac{a-1}{2}$. Each cut contributes to the integrand with a measure μ, and an energy factor E. A triangle filling in between two cuts, represented in Fig. 2, contributes with an interaction that couples the variables on the two cuts. This interaction is factorized into a scalar part $H_{ab}(u,v)$, and matrix part $R_{ab}(\mathbf{i}u - \mathbf{i}v)$ with

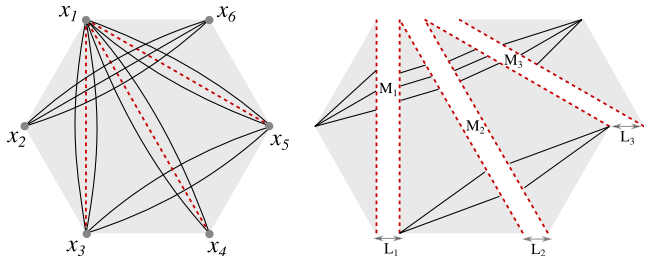

FIG. 1. A 6pt diagram on the plane and its SoV triangulation. There are $L_{i=1,2,3} = 2$ propagators along, and $M_{i=1,3} = 3$, $M_2 = 5$, propagators transverse to the cuts, drawn in red.

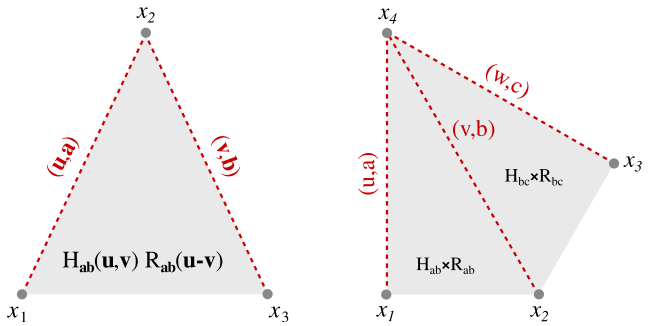

FIG. 2. Left: a tile of the SoV triangulation of a Fishnet integral carrying excitations $(\mathbf{u}, \mathbf{a})$ and $(\mathbf{v}, \mathbf{b})$ on its cuts (red dashed edges). Right: the quadrilateral obtained by gluing two triangles along a common edge.

$\mathbf{i} = \sqrt{-1}$. Bold font notation wants to abbreviate multivariable contributions, which we will make explicit in (5)–(6). Note that $R_{ab} \in \mathrm{End}(V_a \otimes V_b)$, in particular, $R_{ab} \coloneqq (R_{ab})_{ij,kl}$. Note also that the triangles are oriented, indeed $H_{ab}(u,v) \neq H_{ba}(v,u)$.

To read off the spacetime dependence from the triangulation we introduce a pair of cross ratios for any quadrilateral obtained by gluing two triangles that share a cut. With reference to Fig. 2, we define the ratios as

$$Z\bar{Z} = \frac{x_{14}^2 x_{23}^2}{x_{12}^2 x_{34}^2}; \qquad (1-Z)(1-\bar{Z}) = \frac{x_{13}^2 x_{24}^2}{x_{12}^2 x_{34}^2} \tag{3}$$

Any such quadrilateral contributes to the SoV integrand with the factor

$$\otimes_{k=1}^{M} \left[\rho^{\mathbf{i}u_k - \frac{1}{2}} \times e^{\mathbf{i}\theta J_{3,a_k}}\right]; \qquad \begin{matrix} \rho \equiv Z\bar{Z} \\ e^{2\mathbf{i}\theta} = Z/\bar{Z}. \end{matrix}$$

Here $J_{3,a} \in \mathrm{End}(V_a)$ is the generator of rotations on the plane of the n-gon. There is a scalar part, $\rho^{\sum(\mathbf{i}u_k - \frac{1}{2})}$, and matrix part that we denote by $\mathcal{T}_{\underline{\mathbf{a}}}$. Altogether the SoV integrand for a diagram with propagators $\underline{L} = L_1 \ldots L_{n-3}$ and $\underline{M} = M_1 \ldots M_{n-3}$ is given by

$$\mathcal{F}_{\underline{L},\underline{M}} = \prod_{j=1}^{n-3} \mu_{\mathbf{a}_j}(\mathbf{u}_j) \times E_{\mathbf{a}_j}(\mathbf{u}_j)^{L_j + M_j} \times (\rho_j)^{\sum_{k=1}^{M_j}(\mathbf{i}u_{jk} - \frac{1}{2})} \times \prod_{j=2}^{n-3} \mathbf{H}_{\mathbf{a}_{j-1},\mathbf{a}_j}(\mathbf{u}_{j-1}, \mathbf{u}_j) \times \mathcal{T}_{\underline{\mathbf{a}}}[\theta_1, \ldots; \mathbf{u}_1, \ldots] \tag{4}$$

where $\underline{\mathbf{a}} = (\mathbf{a}_1, \ldots, \mathbf{a}_{n-3})$ and we used

$$\mathbf{H}_{\mathbf{a},\mathbf{b}}(\mathbf{u},\mathbf{v}) = \prod_{k=1}^{M}\prod_{h=1}^{N} H_{a_h,b_k}(u_h, v_k)$$

$$E_{\mathbf{a}}(u) = \prod_{m=1}^{M} E_{a_m}(u_m) = \prod_{m=1}^{M} \frac{1}{(u_m^2 + \frac{a_m^2}{4})} \tag{5}$$

The functions μ and H_{ab} are taken from [2,4,6,7] and reported in the Supplemental Material [10] of this letter. The contribution $\mathcal{T}_{\underline{\mathbf{a}}}$ in (4) is the trace on a product of R-matrices

$$\mathbf{R}_{\mathbf{ab}}(\mathbf{u}-\mathbf{v}) = \prod_{k=1}^{M}\prod_{h=1}^{N} R_{a_k b_{N-h+1}}(\mathbf{i}u_k - \mathbf{i}v_{N-h+1}),$$

$$\mathcal{T}_{\underline{\mathbf{a}}} = \mathrm{Tr}_{\underline{\mathbf{a}}}\left[\bigotimes_{\substack{1\le j\le n-3 \\ 1\le m\le M_j}} \left(\frac{Z_j}{\bar{Z}_j}\right)^{J_{3;a_{jm}}} \cdot \prod_{l=2}^{n-3} \mathbf{R}_{\mathbf{a}_{l-1},\mathbf{a}_l}(\mathbf{i}u_{l-1} - \mathbf{i}u_l)\right] \tag{6}$$

where $\mathrm{Tr}_{\underline{\mathbf{a}}} \equiv \mathrm{Tr}_{\mathbf{a}_1} \cdots \mathrm{Tr}_{\mathbf{a}_{n-3}}$ is running over the indices of all the spaces $V_{a_{jm}}$. The matrix $R_{a_h b_k}$ acts as the identity in all other spaces which are not V_{a_k} and V_{b_h}. For example, the expression $R_{ab}R_{ac}$ contains a matrix product only in the

space V_a. Finally, (4) is integrated over rapidities and summed over quantum numbers, i.e.,

$$\mathcal{I}_{\underline{L},\underline{M}} = \sum_{a_1=1}^{\infty} \cdots \sum_{a_M=1}^{\infty} \int du_1 \cdots \int du_M \mathcal{F}_{\underline{L},\underline{M}} \tag{7}$$

The n-point split-ladders are obtained from (4) by setting $L_i \geq 1$ with all the $M_i = 1$. From these, we can think of growing a fishnet of propagators by increasing the $M_i > 1$. The 4-pt representative is $\mathcal{F}_{L_1,M_1}$. As soon as $n \geq 5$, no matter the values of L_i, M_i, the matrix part $\mathcal{T}_{\underline{a}}$ becomes nontrivial.

Strategies and signatures. $\mathcal{F}_{\underline{L},\underline{M}}$ is a meromorphic function of the u_j. Hence, the integration on the real axis in (7) can be performed via Cauchy's theorem by closing the contour with an arc at ∞ for each u_j. The contour is closed in the lower half or the upper half complex plane depending on the kinematical *regions*, $\rho_j < 1$ or $\rho_j > 1$. We encode this in a *signature* $\sigma_j = \pm$. Performing the residue integration accordingly, the result is an expansion of the diagram with the form of a log-stratification

$$\mathcal{I}_{\underline{L},\underline{M}} = \sum_{\{k_i \geq 0\}} \mathbb{F}_{\underline{k}}^{\{\sigma_i\}}(\{Z_i, \bar{Z}_i\}) \times \prod_{j=1}^{n-3} \log^{k_i} \rho_j^{-\sigma_j}, \tag{8}$$

From SoV the task is to obtain all $\mathbb{F}$ coefficient functions. The "maxlog", defined as the $\mathbb{F}$ for which $\sum k_i$ is max, is the same as the light-cone leading log, and therefore plays a special role. Now, since for $n \geq 5$ there are a growing number of signatures, our strategy will be to study a particular one, and perform the integration. Our choice of signature in this letter is $(-, \cdots, -)$, and corresponds to the small-ρ_j expansion. We picked this particular one because it gives rise to a nice recursion w.r.t. the number of external points.

Split-ladders as Mellin-Barnes integrals. The $n$pt split ladders have by definition $M_i = 1$ in (4), and the SoV measure becomes fully factorized wit respect to the pairs (u_j, a_j). This is a situation where standard Mellin-Barnes techniques (MB) can be applied straightforwardly. We shall denote them by $\mathcal{L}_{\underline{L}} \coloneqq \mathcal{F}_{\underline{L},1\ldots,1}$. Within the $(-\cdots-)$ signature it is convenient to change variables from u_j to s_j, as follows,

$$\mathbf{i}u_j = \frac{a_j}{2} + s_j, \tag{9}$$

so that the integrand is "canonical" as a MB integrand:

$$\mathcal{L}_{L_1,\ldots L_{n-3}} = \frac{\rho_1^{s_1}}{\Gamma[1-s_1](-s_1)^{L_1}} \left[\prod_{j=2}^{n-3} \frac{\rho_i^{s_j} \Gamma[s_j - s_{j-1}]}{(-s_j)^{L_j}}\right] \times \frac{\Gamma[-s_{n-3}]\mathcal{T}_{\underline{a}}}{\prod_{i=1}^{n-3}(a_i + s_i)^{L_i}}, \tag{10}$$

where $\Gamma[x]$ is Euler's gamma function and the multi-index is $\underline{a} = (a_1, \ldots, a_{n-3})$. The matrix part reads

$$\mathcal{T}_{\underline{a}} = \frac{\mathcal{P}_{\underline{a}}(Z_1, \bar{Z}_1, \ldots; s_1 \ldots) \prod_j a_j}{\prod_{i=2}^{n-3} \Gamma[1 + a_{j-1} + s_{j-1} - s_j]} \frac{\Gamma[a_1 + s_1]}{\Gamma[1 + a_{n-3} + s_{n-3}]}.$$

and it contains an interesting polynomial $\mathcal{P}_{\underline{a}}$, that we study later in (14). For the moment note that the SoV representation *sequentiates*, see also Fig. 3. Thus the natural way to integrate it is by iteration, starting from s_{n-3}, s_{n-2}, etc. until reaching s_1. By doing so we implicitly assume $\rho_{n-3} < 1$ first, then $\rho_{n-2} < 1$, etc.

We will now see more explicitly how the residue integration is performed according to our choice of signature. In particular, the contour of integration of each s_m variable is simply a vertical line in the complex plane, as standard for Mellin-Barnes integrals. We begin from s_{n-3} by closing the contour so to pick poles from $\Gamma[-s_{n-3}]/(-s)^{L_{n-3}}$. The higher order pole at $s_{n-3} = 0$ is integrated by parts. In any case, derivatives $\partial_{s_{n-3}}$ acting on $\Gamma[s_{n-3} - s_{n-2}]$ are switched to $\partial_{s_{n-2}}$ and further integrated by parts. This pattern continues each time with a slight generalization. In the end, the poles that matter for the integration at step m come from a structure like

$$\oint ds_m (\ldots) \partial_{s_m}^{j_m} \Gamma[s_m - s_{m-1}] \frac{\Gamma[q_{m+1} - s_m]}{(-s_m)^{L_m + i_m}} (\ldots) \tag{11}$$

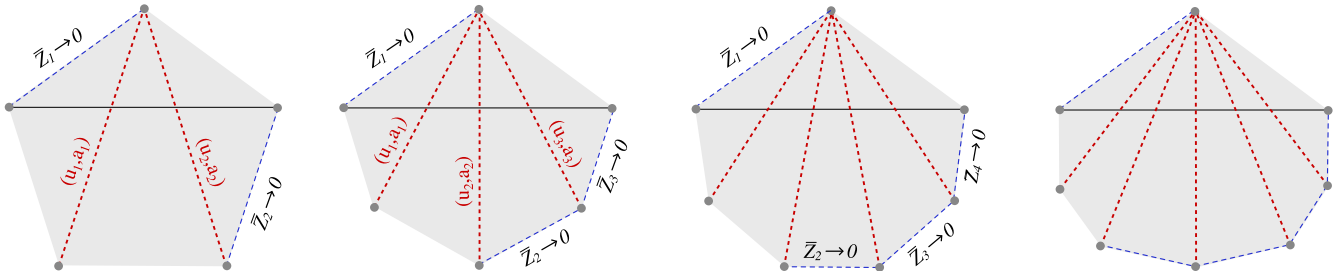

FIG. 3. Split-ladder Feynman diagram in the sequential triangulation. It follows from (3) that the limit $\bar{Z}_k \to 0$ can be realized by sending the dashed blue edges on the light cone. This kinematical region of the Fishnet corresponds to a choice of signature $(-, -, \cdots, -)$ in the integration over SoV rapidities.

where i_m, j_m are integers, and $q_{m+1} = \{0, \mathbb{N}\}$. This structure is similar to that of a split-ladder with fewer external points, therefore we can imagine pictorially that each time we perform an integration, we effectively *eat* a triangular slice from the n-gon as in Fig. 3. Since the pattern repeats, a recursion relation naturally emerges.

Maxlog function and R-matrix at the pole. The maxlogs originate from higher degree poles in $s_j = 0$, upon integration by parts (ibp). Namely, if X and ℓ are generic, the following is true:

$$\int \frac{X}{(-s)^{\ell+1}} = -\int \frac{X}{\ell!}\partial_s^{\ell}\left(\frac{1}{s}\right) \underset{\text{ibp}}{=} \int \frac{(-)^{\ell+1}}{\ell!}\frac{\partial_s^{\ell} X}{s}.$$

A particular maxlog is found when all derivatives hit sequentially the exponent of ρ_j's, producing the term $\prod_j (\log \rho_j)^{L_j}$. This is not the only one we expect: when two base-points of a triangle effectively approach each other, see Fig. 3, propagators lying on different adjacent cuts will pile up, and new contributions are generated. These new contributions come from ibp derivatives in s_j hitting the $\Gamma[s_j - s_{j-1}]$. As a result, the order of the *next* pole, $s_{j-1} = 0$, increases. By taking this into account,

$$\mathcal{I}_{\underline{L}}|_{\text{maxlog}} = \sum_{\substack{0\le i_{n-3}\le L_{n-3} \\ 0\le i_2 \le \dots \le L_2 + j_{(3)}}} \mathbb{F}^{-\cdots-}_{i_1,\dots,i_{n-3}}(\{Z_i, \bar{Z}_i\}) \prod_{k\ge 1} \log^{i_k}\rho_k,$$

where $i_1 = L_1 + j_{(1)}$ and $j_{(k)} = \sum_{m>k}(L_m - i_m)$. An explicit computation shows that maxlogs are an evaluation formula at $s_j = 0$ that we can write as

$$\mathbb{F}^{-\cdots-}_{i_1,\dots,i_{n-3}} = \sum_{\underline{a}} \frac{\mathcal{T}_{\underline{a}}(0)}{\prod_{k\ge 1} a_k^{L_k}} \times \prod_{k\ge 1} \frac{(-)^{L_k+1}}{i_k!}, \tag{12}$$

$$\mathcal{T}_{\underline{a}}(0) = \mathcal{D}^{(a_{n-3})}_{n-3,n-2} \dots \mathcal{D}^{(a_2)}_{2,1}\left[\frac{W_1^{a_1} - \bar{W}_1^{a_1}}{W_1 - \bar{W}_1}\right], \tag{13}$$

in term of the operators (2), where $W_1 = Z_1$, $\bar{W}_1 = \bar{Z}_1$, and $W_{i\ge 2} = Z_i W_{i-1}$, similarly for $\bar{W}_{i\ge 2}$. Nicely enough, the sum over $a_1 \in \mathbb{N}$ in (12) can be done, and yields the right-hand side (rhs) of formula (1). Note that the split-ladders are pure transcendental functions of $(Z_i, \bar{Z}_i)$, multiplied by a rational prefactor, i.e., the leading discontinuity. From the maxlog we find that the latter is $(W_{n-3} - \bar{W}_{n-3})^{-1} = (\prod Z_i - \prod \bar{Z}_i)^{-1}$. This fact has been checked independently from the Feynman representation of the diagram, see eg. [18,19].

Twisted traces and polynomials. The SoV representation provides concrete formulas for any coefficient function in (8), not just the maxlogs. The only complication comes from the R-matrix and the polynomial

$$\mathcal{P}_{\underline{a}} = \rho_1^{\frac{a_1-1}{2}} \prod_{i=2}^{n-3} (-1)^{a_i - 1} (\rho_i)^{\frac{a_i - 1}{2}} \times \text{Tr}_{\underline{a}}\left[\bigotimes_{1\le j\le n-3} \left(\frac{Z_j}{\bar{Z}_j}\right)^{J_{3;a_j}} \cdot \prod_{l=2}^{n-3} R_{a_{l-1},a_l}\right]. \tag{14}$$

Nicely enough, we have found an explicit formula for this trace. Let us introduce first,

$$r_{ai;bj}(U) = \sum_{k\ge 0} (1+j-a+i-U)_{b-1-j-k}(a-i)_k \times \frac{(k-U-i)_{j-k}(b-j-k)_k (1+i-k)_k (1+j-k)_k}{(k!)^2},$$

where $(x)_a = \Gamma[x+a]/\Gamma[x]$. Then, the simplest 5pt case, $\mathcal{P}_{ab}$, is given by

$$\mathcal{P}_{ab} = \sum_{i=0}^{a-1}\sum_{j=0}^{b-1} r_{ai,bj}(U_{12}) Z_1^i Z_2^j \bar{Z}_1^{a-1-i} \bar{Z}_2^{b-1-j}, \tag{15}$$

with $U_{12} \equiv s_1 - s_2$. Here the sum over $Z^{\#_1}\bar{Z}^{\#_2}$ runs over the eigenvalues of $J_{3;a}, J_{3;b}$. The generalization to higher points is straightforward,

$$\mathcal{P}_{\underline{a}} = \sum_{\substack{j_1\le a_1-1 \\ \dots \\ j_{n-3}\le a_{n-3}-1}} \prod_{k=2}^{n-3} r_{a_{k-1}j_{k-1},a_k j_k}(U_{k-1,k}) Z_1^{j_1} \dots \bar{Z}_1^{a_1-1-j_1} \dots,$$

and works upon checking on (many) explicit examples.

Cauchy identity tool for multipoint fishnets. The crucial novelty for fishnets, with respect to split-ladders, is the nonfactorizable measure. To deal with it systematically, we use the dual Cauchy identity for Schur polynomials $P_{\underline{\lambda}}$, see, e.g., [20], and rewrite the measure as

$$\mu_{\mathbf{a}}(\mathbf{u}) = \frac{\text{VdM}(\mathbf{s})\text{VdM}(\mathbf{s}+\mathbf{a})}{(2\pi\mathbf{i})^M M!} \sum_{\underline{\lambda}\subseteq M^M} P_{\underline{\lambda}}(\mathbf{s}) P_{\underline{\lambda}^c}(\mathbf{s}+\mathbf{a}).$$

Here, $\text{VdM}(\mathbf{s})$ is the VanderMonde of variables $s_{i=1,\dots M}$, whereas $\underline{\lambda}, \underline{\lambda}^c$ are two conjugate partitions of M^M. From here the residue integration becomes quite more transparent. First, note that $\text{VdM}(\mathbf{s})P(\mathbf{s})$ is itself a determinant, thus when acted upon by derivatives from ibp, it vanishes in $\mathbf{s} = 0$ unless the derivatives are distributed as $\partial_{s_i}^{\#_i}$ with $\#_i = \lambda_i + (i-1)$ or permutations thereof. Consider now the jth cut. Each $E_{\mathbf{a}_j}(\mathbf{u}_j)^{L_j+M_j}$ energy factor produces $M_j - 1 + L_j$ derivatives ∂_{s_i} from ibp for each $i = 1, \dots, M_j$. The minimal set of ibp derivatives that the measure can absorb corresponds to $\underline{\lambda} = \varnothing$, for which $P_{\varnothing} = 1$ and $\varnothing^c = [M_j, \dots, M_j]$. We find that for each of the s_i a number $(M_j - 1)/2 + L_j$ of derivatives distribute antisymmetrically on $P_{[M_j,\dots,M_j]}(\mathbf{s}_j + \mathbf{a}_j) \times \text{VdM} \times \rho_j^{\mathbf{s}} \times \mathbf{H}_{\mathbf{a},\mathbf{b}} \times \mathcal{T}_{\underline{\mathbf{a}}}$. From combinatorics it follows that $(\log \rho_j)^{M_j L_j}$ is the

maximal power of $\log\rho_j$. The remaining derivatives, in number $(M_j-1)/2$ for each of the s_i, with $i=1,\ldots,M_j$, and for all $j=1,\ldots n-3$, will act on the rest of the integrand, ie. factors $P_{[M_j,\ldots,M_j]}(\mathbf{s}_j+\mathbf{a}_j)\times\mathrm{VdM}$ and $\mathbf{H}_{\mathbf{a},\mathbf{b}}\times\mathcal{T}_{\underline{\mathbf{a}}}$, and an expression for the maxlog coefficient function follows. A similar analysis generalizes to $\underline{\lambda}\neq\varnothing$.

In the special case of the 4pt fishnets there is only a cut and so the maxlog is given by ibp derivatives acting on $P_{[M_1,\ldots,M_1]}(\mathbf{s}+\mathbf{a})\times\mathrm{VdM}$. Hence, a determinantal formula for the maxlog follows immediately by construction; and by imposing Steinmann relations as in [7] one can straightforwardly lift this maxlog determinant and obtain a version of the Basso-Dixon result.

Stampedes. In planar and light-cone kinematics we can combine SoV results with *stampedes* technique. Let $S_j=\{j,\ldots j+m_j\}$ be a collection of consecutive indices, for $j\in P\subset\{1,\ldots,n\}$. We consider the regime where points in S_j approach a light-ray, that is $x_{i\in S_j}=(w_{i\in S_j},\bar{w}_j)$ in light-cone coordinates, and look at the leading behavior of the diagram. For an n-pt fishnet we then expect a generalized Taylor expansion of the form

$$\mathcal{I}_{M\times L}=\sum_{\substack{|\underline{k}|=ML\\ \underline{J}\geq 0}}\left[\left(\prod_{j\in P}\lambda_j^{k_j}\prod_{i\in S_j,i\neq j}w_{i,j}^{J_i}\right)\mathbf{f}_{\underline{k};\underline{J}}(\eta,\bar{\eta})+\cdots\right]+\cdots \tag{16}$$

where $\lambda_j\sim-\log\bar{w}_{i,j}$. The functions $\mathbf{f}_{k_1,\ldots,k_p;\underline{J}}$ carry the leftover coordinate dependence, denoted collectively as $(\eta,\bar{\eta})$. For (16) to hold, any vertex of the diagram has to be the intersection of two lines emitted from external points x_i, x_k such that $\exists\, j\in P|i,k\in S_j$.

We are going to show that the $\mathbf{f}_{k_1,\ldots,k_p;\underline{J}}$ are generated via combinatorics. First, fields that become null-separated, e.g. $\phi(x_j),\phi'(x_{j+1})$ for $j\in P$, are replaced by a Taylor expansion along a light-ray. Doing so, we create states $|\mathrm{in}(J)\rangle_j$ obtained from inserting light-cone derivatives $\hat{\partial}^n\equiv\partial^n/n!$ between a number R and R' of fields emitted from the points x_j and x_{j+1},

$$(\phi_1\cdots\phi_R)(x_j)\hat{\partial}^J(\phi'_1\cdots\phi'_{R'})(x_j)|\mathrm{vacuum}\rangle=|\mathrm{in}(J)\rangle_j \tag{17}$$

as in FIG. 4. Last formula becomes $|\mathrm{in}(J_1,J_2,J_3,\ldots)\rangle_j$ when also fields $\phi''(x_{j+2}),\phi'''(x_{j+3}),\ldots$ are expanded around x_j. Next, we will generate loop corrections by acting on these states with the one-loop dilations $\mathbb{H}_i$ at position x_i. Each ϕ is one of the fields $\mathcal{X},\bar{\mathcal{X}}$ or $\mathcal{Z},\bar{\mathcal{Z}}$ in the fishnet CFT [4,21], whose propagators are rows/columns of the fishnet diagram. The action of $\mathbb{H}_i$ is

$$\mathbb{H}_i|\hat{\partial}^{h_1}\phi_1\ldots\hat{\partial}^{h_R}\phi_R\rangle_i=\sum_{k=1}^{R-1}\mathbb{h}_{k,k+1}|\hat{\partial}^{h_1}\phi_1\ldots\hat{\partial}^{h_R}\phi_R\rangle_i$$

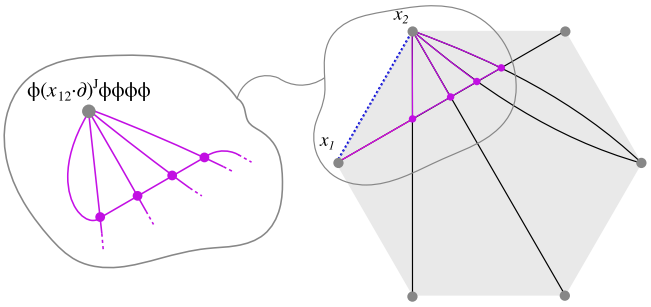

FIG. 4. The signature $(-,-,-)$ captures explicitly the $\log^4\rho_1$ behavior of the six-point ladder with $L_{i=1,2}=1$ and $L_3=2$ in the limit $x_{12}^2\to 0$. Here, the displacement between fields at x_1, x_2 is replaced by the expansion $\mathrm{Tr}[\phi(x_1)(x_{12}^\mu\partial_\mu)^J\phi(x_1)^4]$.

where

$$\mathbb{h}_{12}|\hat{\partial}^{h_1}\mathcal{X},\hat{\partial}^{h_2}\mathcal{Z}\rangle_i=\sum_{j+l=h_1+h_2}\frac{|\hat{\partial}^j\mathcal{Z},\hat{\partial}^l\mathcal{X}\rangle_i}{h_1+h_2+1}. \tag{18}$$

Other nonzero matrix elements are obtained by cyclic permutations $\mathcal{X}\to\mathcal{Z}\to\bar{\mathcal{X}}\to\bar{\mathcal{Z}}$. In particular, states with opposite *chirality* are annihilated $\hat{h}_{12}|\hat{\partial}^n\mathcal{Z},\hat{\partial}^m\mathcal{X}\rangle=0$.

At this point, $\mathbf{f}_{k_1,\ldots,k_p;J}$ is the monomial of degree $(k_1,\ldots,k_p)$ in the "times" λ_j, of the generating function

$$\begin{aligned}\mathcal{G}_{\underline{J}}(\lambda_j)&=\mathbf{C}\cdot e^{\sum_{i\in P}\lambda_i\mathbb{H}_i}|\mathrm{in}(\underline{J})\rangle,\\ |\mathrm{in}(\underline{J})\rangle&=\bigotimes_{\substack{i\in\{1,\ldots,n\}\setminus S\\ S=\cup_j S_j\setminus\{j\}}}|\mathrm{in}(\underline{J_i})\rangle_i\end{aligned} \tag{19}$$

The initial state is given by (17) whenever $i\in P$,

$$|\mathrm{in}(\underline{J_i})\rangle_i\equiv|\mathrm{in}(J_{h_1},\ldots,J_{h_{m_i-1}})\rangle_i,$$

otherwise $\underline{J_i}=\underline{0}$ for $i\notin P$. Finally, the functional $\mathbf{C}$ is the free-theory contraction of fields $\phi_i(y_i)$ and $\phi'_i(y'_i)$ that stand at endpoints of a given line in the fishnet lattice.

For example, take a 4-pt fishnet with $S_1=\{1,2\}$;

$$\mathbf{f}_{ML,J}=\frac{1}{\prod_{h=1}^{L}\prod_{k=1}^{M}(M+L-h-k+1)}\times\mathbb{F}_{M,L}(J), \tag{20}$$

where $\mathbb{F}_{M,L}(J)$ is the canonical partition function of a vertex model on a square-lattice of size $M\times L$, with J excitations, Boltzmann weights

$$V(a,b;c,d)=\frac{\delta_{a+b,c+d}}{a+b+1},$$

and domain-wall boundary conditions as in Fig. 5. From this description, the maxlog in (16) is the grand canonical partition function of the above vertex-model with fugacity $Z=w_{12}w_{34}/w_{14}w_{23}$. The *zero-temperature* pre-factor in (20) was computed in [9] as the euclidean operator product expansion limit $Z\to 0$. The same vertex model describes maxlogs for higher-pt partition functions.

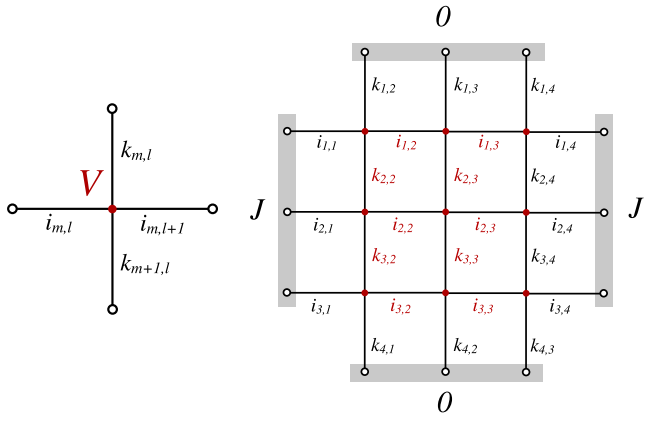

FIG. 5. The vertex model for $\mathbf{f}_{ML,J}$ with $M = L = 3$. Indices $i_{m,l}$ and $k_{m,l}$ are summed over in the bulk, and constrained along boundaries. Vertically, $\sum_{m=1}^{M} i_{m,1} = J = \sum_{m=1}^{M} i_{m,L+1}$. Horizontally $k_{1,l} = k_{M+1,l} = 0$.

Conclusions and outlook. We initiated a systematic study of multi-point Feynman integrals at any-loop order in planar kinematics, by combining integrability/SoV methods [2,4,6,22], with Mellin space and symmetric polynomials techniques. We first solved a class of point-split ladder integrals by an elegant recursion, and then for n-point fishnets, we introduced a Cauchy identity representation of the SoV measure, showing how this could be used to understand the pattern of emergent structures.

Some future directions. Our results apply directly to Fishnet CFTs, a family of integrable 4d theories closely related to $\mathcal{N} = 4$ SYM [21,23,24], where it is known that all Feynman diagrams ultimately should be related to partition functions of an integrable lattice model [25]. Throughout our discussion we have indeed provided concrete realizations of this statement. But in addition, fishnet diagrams describe conformal correlators and can be considered as a simplified playground to familiarize with CFT/integrability tools for multipoint correlators, e.g., [26–32]. In this respect, beyond one-loop, not much is known about multi-point conformal integrals and the space of functions they describe, see [33–37] for recent progress. An intriguing direction would be to bootstrap the diagrams we discussed here by combining 1) data from the SoV log stratification, 2) an ansatz in terms of pure functions (such as [38–42]) and 3) analytic constraints (single-valuedness, Steinmann relations [43,44], etc.). We expect integrability to imply simple structures at any loop order, generalizing nontrivially the determinants found by [6]. Finally, it would be interesting to lift our methods out of the plane, and extend the use of SoV technique to multi-point conformal integrals with other topologies, but similar analytic properties.

Acknowledgments. We thank James Drummond for discussions and for providing us the symbol of $\mathcal{L}_{1,1}$, and Ömer Gürdogan for helping us integrating the symbol. We also thank Frank Coronado, Paul Heslop and Pedro Vieira for very helpful comments. Research at Perimeter Institute is supported in part by the Government of Canada through the Department of Innovation, Science, and Economic Development Canada and by the Province of Ontario through the Ministry of Colleges and Universities. F. A. is supported by the Ramon y Cajal program through the fellowship RYC2021-031627-I funded by MCIN/AEI/10.13039/501100011033 and by the European Union NextGenerationEU/PRTR. Finally, we acknowledgment the FAPESP Grants No. 2019/24277-8 and No. 2020/16337 for support during our stay at the ICTP South American Institute for Fundamental Research, Instituto de Física Teórica-UNESP, in Sao Paulo, where part of this work was done.

[1] R. P. Feynman, The theory of positrons, Phys. Rev. **76**, 749 (1949).
[2] E. Olivucci, Hexagonalization of fishnet integrals II: Overlaps and multi-point correlators, arXiv:2306.04503.
[3] J. M. Maillet and G. Niccoli, On quantum separation of variables beyond fundamental representations, SciPost Phys. **10**, 026 (2021).
[4] S. Derkachov and E. Olivucci, Exactly solvable magnet of conformal spins in four dimensions, Phys. Rev. Lett. **125**, 031603 (2020).
[5] S. Derkachov and E. Olivucci, Exactly solvable single-trace four point correlators in χCFT$_4$, J. High Energy Phys. 02 (2021) 146.
[6] B. Basso, J. Caetano, and T. Fleury, Hexagons and correlators in the fishnet theory, J. High Energy Phys. 11 (2019) 172.
[7] B. Basso and L. J. Dixon, Gluing Ladder Feynman diagrams into fishnets, Phys. Rev. Lett. **119**, 071601 (2017).
[8] B. Basso, L. J. Dixon, D. A. Kosower, A. Krajenbrink, and D. l. Zhong, Fishnet four-point integrals: Integrable representations and thermodynamic limits, J. High Energy Phys. 07 (2021) 168.
[9] E. Olivucci and P. Vieira, Stampedes I: Fishnet OPE and octagon Bootstrap with nonzero bridges, J. High Energy Phys. 07 (2022) 017.
[10] See Supplemental Material at http://link.aps.org/supplemental/10.1103/PhysRevD.108.L121902 for the technical reviews of a few definitions and further details and examples concerning the derivation of the results presented in the letter, organized in 7 Secs. I–VII.

[11] P. P. Kulish, N. Y. Reshetikhin, and E. K. Sklyanin, Yang-Baxter equation and representation theory. 1., Lett. Math. Phys. **5**, 393 (1981).
[12] O. A. Castro-Alvaredo and J. M. Maillet, Form factors of integrable Heisenberg (higher) spin chains, J. Phys. A **40**, 7451 (2007).
[13] B. Basso and D. l. Zhong, Continuum limit of fishnet graphs and AdS sigma model, J. High Energy Phys. 01 (2019) 002.
[14] James Drummond (private communication).
[15] Don Zagier, The Dilogarithm Function notes available at https://maths.dur.ac.uk/users/herbert.gangl/dilog.pdf.
[16] N. I. Usyukina and A. I. Davydychev, An approach to the evaluation of three and four point ladder diagrams, Phys. Lett. B **298**, 363 (1993).
[17] A. P. Isaev, Multiloop Feynman integrals and conformal quantum mechanics, Nucl. Phys. **B662**, 461 (2003).
[18] F. Cachazo, Sharpening the leading singularity, arXiv: 0803.1988.
[19] J. Drummond, C. Duhr, B. Eden, P. Heslop, J. Pennington, and V. A. Smirnov, Leading singularities and off-shell conformal integrals, J. High Energy Phys. 08 (2013) 133.
[20] I. G. Macdonald, *Symmetric Functions and Hall Polynomials*, 2nd ed. (Oxford University Press, New York, 1994).
[21] Ö. Gürdoğan and V. Kazakov, New integrable 4D quantum field theories from strongly deformed planar $\mathcal{N} = 4$ supersymmetric Yang-Mills theory, Phys. Rev. Lett. **117**, 201602 (2016).
[22] E. Olivucci, Hexagonalization of Fishnet integrals. Part I. Mirror excitations, J. High Energy Phys. 11 (2021) 204.
[23] J. Caetano, Ö. Gürdoğan, and V. Kazakov, Chiral limit of $\mathcal{N} = 4$ SYM and ABJM and integrable Feynman graphs, J. High Energy Phys. 03 (**2018**) 077.
[24] N. Gromov, V. Kazakov, G. Korchemsky, S. Negro, and G. Sizov, Integrability of conformal fishnet theory, J. High Energy Phys. 01 (2018) 095.
[25] A. B. Zamolodchikov, Fishnet diagrams as a completely integrable systems, Phys. Lett. B **97**, 63 (1980).
[26] V. Rosenhaus, Multipoint conformal blocks in the comb channel, J. High Energy Phys. 02 (2019) 142.
[27] I. Buric, S. Lacroix, J. A. Mann, L. Quintavalle, and V. Schomerus, From Gaudin integrable models to d-dimensional multipoint conformal blocks, Phys. Rev. Lett. **126**, 021602 (2021).
[28] D. Poland and V. Prilepina, Recursion relations for 5-point conformal blocks, J. High Energy Phys. 10 (2021) 160.
[29] I. Buric, S. Lacroix, J. A. Mann, L. Quintavalle, and V. Schomerus, Gaudin models and multipoint conformal blocks: general theory, J. High Energy Phys. 10 (2021) 139.
[30] I. Buric, S. Lacroix, J. A. Mann, L. Quintavalle, and V. Schomerus, Gaudin models and multipoint conformal blocks. Part II. Comb channel vertices in 3D and 4D, J. High Energy Phys. 11 (**2021**) 182.
[31] I. Buric, S. Lacroix, J. A. Mann, L. Quintavalle, and V. Schomerus, Gaudin models and multipoint conformal blocks III: Comb channel coordinates and OPE factorisation, J. High Energy Phys. 06 (2022) 144.
[32] A. Kaviraj, J. A. Mann, L. Quintavalle, and V. Schomerus, Multipoint lightcone bootstrap from differential equations, J. High Energy Phys. 08 (2023) 011.
[33] D. Chicherin, J. Drummond, P. Heslop, and E. Sokatchev, All three-loop four-point correlators of half-BPS operators in planar $\mathcal{N} = 4$ SYM, J. High Energy Phys. 08 (2016) 053.
[34] D. Chicherin, V. Kazakov, F. Loebbert, D. Müller, and D. l. Zhong, Yangian symmetry for fishnet Feynman graphs, Phys. Rev. D **96**, 121901 (2017).
[35] H. S. Hannesdottir, A. J. McLeod, M. D. Schwartz, and C. Vergu, Constraints on sequential discontinuities from the geometry of on-shell spaces, J. High Energy Phys. 07 (2023) 236.
[36] A. McLeod, R. Morales, M. von Hippel, M. Wilhelm, and C. Zhang, An infinite family of elliptic ladder integrals, J. High Energy Phys. 05 (2023) 236.
[37] A. J. McLeod and M. von Hippel, Traintracks all the way down, arXiv:2306.11780.
[38] A. B. Goncharov, Multiple polylogarithms and mixed Tate motives, arXiv:math/0103059.
[39] O. Schnetz, Graphical functions and single-valued multiple polylogarithms, Commun. Num. Theor. Phys. **8**, 589 (2014).
[40] E. Panzer, Feynman integrals and hyperlogarithms, arXiv: 1506.07243.
[41] J. Broedel, C. Duhr, F. Dulat, B. Penante, and L. Tancredi, Elliptic polylogarithms and Feynman parameter integrals, J. High Energy Phys. 05 (**2019**) 120.
[42] Stefan-Gheorghe Druc and James M. Drummond, Amplitudes in $\mathcal{N} = 4$ super Yang-Mills, Ph.D. thesis, University of Southampton, available at https://eprints.soton.ac.uk/428038/1/Final_Thesis.pdf.
[43] O. Steinmann, Helv. Phys. Acta **33**, 257 (1960); Phys. Acta **33**, 347 (1960).
[44] S. Caron-Huot, L. J. Dixon, A. McLeod, and M. von Hippel, Bootstrapping a five-loop amplitude using Steinmann relations, Phys. Rev. Lett. **117**, 241601 (2016).